Self organized spatio-temporal structure within the fractured Vadose Zone: The influence of dynamic overloading at fracture intersections

Randall A. LaViolette
Idaho National Engineering & Environmental Laboratory, Idaho Falls, Idaho, USA

Robert J. Glass
Sandia National Laboratories, Albuquerque, New Mexico, USA

Received 2 June 2004; revised 29 July 2004; accepted 19 August 2004; published 23 September 2004.

[1] Under low flow conditions (where gravity and capillary forces dominate) within an unsaturated fracture network, fracture intersections act as capillary barriers to integrate flow from above and then release it as a pulse below. Water exiting a fracture intersection is often thought to enter the single connected fracture with the lowest invasion pressure. When the accumulated volume varies between intersections, the smaller volume intersections can be overloaded to cause all of the available fractures exiting an intersection to flow. We included the dynamic overloading process at fracture intersections within our previously discussed model where intersections were modeled as tipping buckets connected within a two-dimensional diamond lattice. With dynamic overloading, the flow behavior transitioned smoothly from diverging to converging flow with increasing overload parameter, as a consequence of a heterogeneous field, and they impose a dynamic structure where additional pathways activate or deactivate in time. *INDEX TERMS:* 1848 Hydrology: Networks; 1875 Hydrology: Unsaturated zone; 1869 Hydrology: Stochastic processes. **Citation:** LaViolette, R. A., and R. J. Glass (2004), Self organized spatio-temporal structure within the fractured Vadose Zone: The influence of dynamic overloading at fracture intersections, *Geophys. Res. Lett.*, *31*, L18501, doi:10.1029/2004GL020659.

1. Introduction

[2] Unsaturated flow experiments in fracture networks indicate that intersections can direct flow to a single exiting fracture [*LaViolette et al.*, 2003]. In addition, they have been found to gather water from above to release as a pulse below [*Wood et al.*, 2002]. Recently we employed a simple automaton to study the consequences of these two fracture intersection behaviors embedded within a network [*Glass and LaViolette*, 2004, hereinafter referred to as I]. This "tipping bucket model" or TBM is similar to the generic directed "sand-pile" model originally studied by *Dhar and Ramaswamy* [1989] but with the added complication of stochastic, singly directed flow. The TBM idealizes the fracture network as a regular, two-dimensional array of intersections arranged on a diamond lattice (Figure 1). Periodic boundary conditions are implemented along the vertical edges of the network of 100 (horizontal) $\times$ 1000 (vertical) sites, so that water exiting on one side reappears on the other. Buckets are placed on alternate sites on the horizontal axis so that there are 50 buckets on each row. Φ is defined as the fraction of intersections, or buckets, that are connected to only one or the other but not both of the neighboring buckets in the row below. For $\Phi > 0$, the choice of which of the two neighboring buckets to connect is random; once chosen, it remained set for the duration of the simulation. Water is added in unit increments at random to buckets along the top row and exits the network from the bottom row. Between additions, the network is relaxed by tipping the eligible buckets, as follows: when the level of water in a bucket j exceeds its threshold θ_j (which in I were all set to 10), it tips and distributes all of its volume to the (one or two) connecting buckets in the row below; the direction of the flow is always top to bottom. We obtain from operation of these simple local rules a self-organized spatial-temporal structure. For increasing Φ, channels form due to convergence within the network; spatial structure with depth transitioned from divergent to braided to the fully convergent hierarchal end member at $\Phi = 1$. Water moves through these defining structures as pulses, or avalanches, that can penetrate to great depths. The avalanche size distribution transitions away from power-law behavior as Φ increases and convergence breaks the scaling. For only single outflow ($\Phi = 1$), convergence is maximal and every avalanche spans the entire system but transmits the minimum volume of water.

[3] Here, we extend the TBM to consider the added realism of the dynamic overload process. Dynamic overloading occurs when a large volume of fluid is passed to a small volume intersection and causes the bucket to split its flow even if normally it would only direct the flow singly. We consider this additional process in context of a heterogeneous bucket field as is also expected in natural fracture networks. We find that as occurrence of dynamic overloading increases, the model behavior transitions from convergent flow back to divergent flow comparably to that found in I for Φ. The position of the transition is dependent on the width

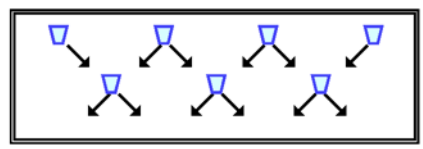

Figure 1. Network of fracture intersections represented by buckets. For $\Phi = 0$, each bucket connects to exactly two on the row above and two on the row below. For $\Phi > 0$, one arrow leaving a bucket may be removed. For $\Phi = 1$, all buckets have one arrow in and one arrow out.

0094-8276/04/2004GL020659$05.00

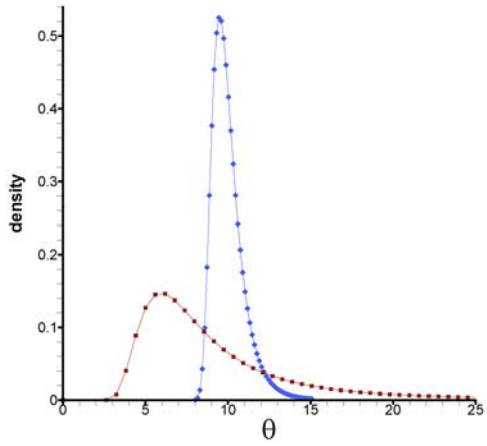

Figure 2. The "narrow" (blue with solid diamonds) and the "wide" (red with solid squares) density distributions, respectively, of the bucket threshold θ.

of the distribution and can be roughly scaled by its coefficient of variation. The divergent flow with overloading differs from that for Φ as it occurs as a natural consequence of a heterogeneous field and imposes a dynamic structure where additional pathways activate or deactivate in time.

2. Dynamic Overload Simulations

[4] In the TBM, a fracture intersection is treated as a capillary barrier from which two fractures depart to connect to neighboring intersections. Water can enter the pool (bucket) above the intersection from either of the two connected intersections above. As the volume increases, the pressure builds at the intersection and eventually the threshold (i.e., pressure at the intersection) for entering the capillary barrier is reached. When the capillary barrier fails, only one of the fractures is likely to be invaded, as the invasion pressure for each will be different. Such low flow behavior generates slender plumes as has been found experimentally [*Glass et al.*, 2003a, 2003b] and simulated using modified invasion percolation models, even without considering fracture intersections as capillary barriers [*Glass et al.*, 2004]. However, the pressure at the intersection can be pushed above the invasion pressure of the barrier if a large volume of water is passed from above and causes the pool height to rise above the minimal height required for breach. When this happens, increased pressure at the intersection allows fluid to exceed the entry pressure of both fractures and thus flow will be split.

[5] To model the overload process, we added a second threshold condition at each bucket through introduction of the overload parameter $\Omega \geq 1$ constant for the entire network. For each bucket j, if the bucket receives a load L_j that is larger than θ_j by a factor of Ω, i.e., if $L_j > \Omega\, \theta_j$, then the restriction to flow into only one bucket below (if any) is overridden for that instance only, so that both of the left and right connecting buckets below equally receive $\frac{1}{2} L_j$ from j.

[6] In context of overloading, the added realism of variable bucket threshold within the network is useful. The θ_j here were assigned to each bucket (to remain fixed thereafter), without spatial correlation, by randomly sampling from the Fréchet distribution. This distribution, a

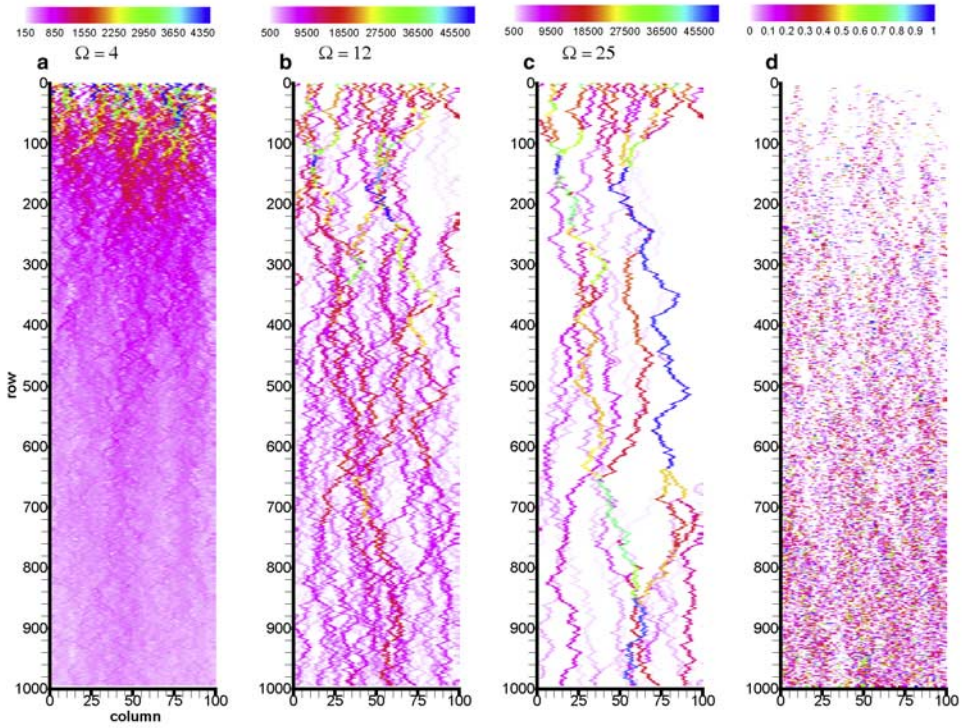

Figure 3. Distribution of flow for three choices of the overload parameter Ω. The left (a), center (b), and right (c) panels show the accumulated number of times a bucket has been tipped with Ω = 4, 12, and 25, respectively. The far right (d) panel shows the ratio of the number of times a bucket was overloaded to the number of times it was tipped for Ω = 12. Each result is for the "wide" threshold distribution.

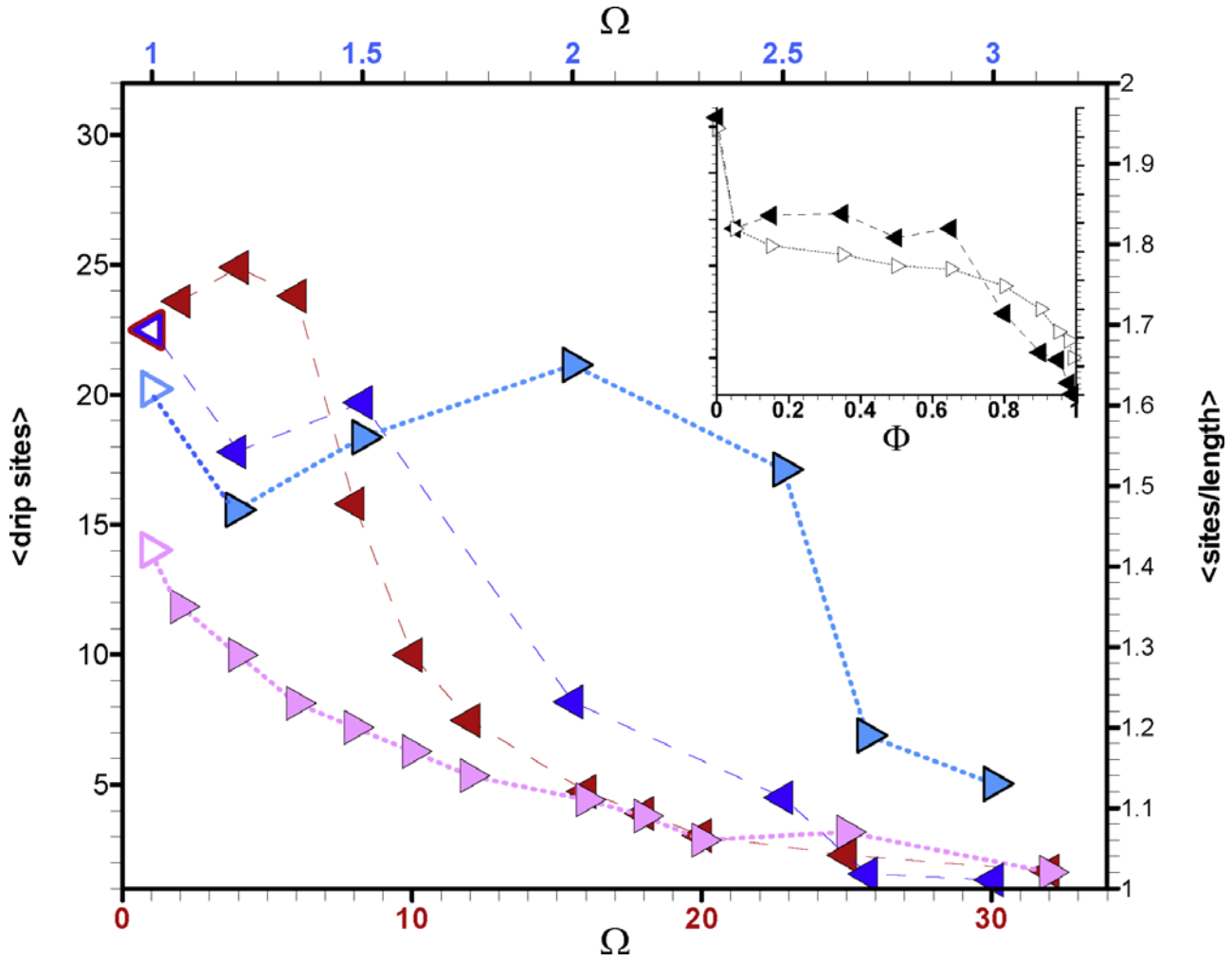

Figure 4. Two measures of flow convergence. The left scale shows the mean number of buckets in the bottom row employed in each drip event; the left-hand triangles correspond to the left scale. The right scale shows the mean of the number of sites divided by the length of each avalanche; the right-hand triangles correspond to the right scale. The main panel shows the variation of both with respect to the overloading parameter Ω with $\Phi = 1$. Both sets of red triangles are read from the bottom scale, corresponding to Ω for the "wide" distribution. Both sets of blue triangles are read from the top scale, corresponding to Ω for the "narrow" distribution. The closed symbols correspond to $\Omega > 1$; the open red or blue triangles correspond to $\Omega = 1$. The inset shows for comparison (from paper I) the variation of both with respect to Φ, for constant threshold and no overloading. The left and right scales are identical to those of the main panel. The dashed lines in either panel are only guides to the eye.

member of the "generalized extreme value" family of distributions [*Coles*, 2001], is unimodal, possesses a positive skew (which is often observed for measured fracture aperture distributions) and happens also to have convenient scaling properties. Its essential singularity at the origin ensures a smooth, rapid approach to zero density there. Its algebraic decay for large thresholds is both physical [*Bonnet et al.*, 2001] and convenient in that it permits especially wide as well as narrow distributions. Its two parameters were set by specifying both the mean threshold (μ_θ) and its standard deviation (σ_θ) for each of two cases: a "wide" ($\sigma_\theta = 10$) and a "narrow" ($\sigma_\theta = 1$) distribution. In both cases we set $\mu_\theta = 10$, in correspondence with I. The two choices for σ_θ were made to bracket our guess for the variation that would be found in natural fractured rock; experiments on fracture aperture distributions suggest that the closely related threshold distribution might be even wider than our "wide" case [*Bonnet et al.*, 2001]. Figure 2 shows the distribution for these two cases.

3. Results and Discussion

[7] Each simulation was driven by 8×10^6 unit additions, (following the first 10^6 additions that were discarded), Φ was set to unity, and Ω set to a fixed value chosen from a range from unity, where the $\Phi = 0$ results were recovered, to sufficiently large values, where overloading was absent. For increasing Ω, the region swept by avalanches over the course of an entire simulation transitions from the fully divergent $\Phi = 0$ result through a braided to the fully convergent regime. Images of the number of times a bucket tips over the course of a simulation are shown in Figure 3 for a single realization of the wide distribution bucket network and Ω of 4, 12, and 25. Flow structures transition

from primarily single bucket wide pathways at $\Omega = 25$ (near the fully convergent $\Phi = 1$ result) to primarily diffuse plumes at Ω of 4. This transition is similar to that found in I for Φ (see their Figure 3). Locations where occasional overloading causes the formation of an ephemeral flow path can be easily seen in Figure 3c ($\Omega = 25$) as cooler colors emanating from buckets that split flow. For $\Omega = 12$ (Figure 3b), many such overloading events occur to create a braided structure. Figure 3d shows the ratio of the number of times a bucket is overloaded to the number of times the bucket tips over the course of this simulation ($\Omega = 12$). We also see in Figure 3, for each Ω, a transition from converging to diverging flow with depth, the smaller Ω the quicker the transition. This occurs because overloading is dependent on having a large bucket above a smaller one (j) such that the size of the load passed must exceed $\Omega\theta_j$, and the probability for this to occur increases with depth and with decreasing Ω.

[8] In Figure 4 we display the behavior of two measures: first, anticipating experiments that might actually be (but have not yet been) performed on opaque systems, we examine the average number of exiting fractures where water leaves the network at its bottom (left axis); second, we look inside the flow itself, and consider avalanche shape by measuring the ratio of the number of buckets tipped in an avalanche event to the depth of event penetration (i.e., the number of contiguous rows) (right axis). We also have plotted (inset) the same measures for I with variation of Φ to demonstrate that the behavioral response for Ω is indeed very similar as for Φ alone. The difference in sensitivity to Ω for the two-bucket size distributions is quite dramatic. In Figure 4 we have scaled the axes for Ω (i.e., wide and narrow distributions) to capture the appropriate variations in a single plot. The narrow and wide distribution scales are different by factor of about 10, the same as between the coefficient of variation for the two distributions. Such scaling is similar to that found in other analyses that weigh the influence of random variation to an organizing influence such as is represented by the overloading process here [e.g., *Glass et al.*, 2003a, 2003b]. Beyond this gross scaling, differences remain in Figure 4 that are intrinsically related to the influence of the bucket size distribution itself. There is a systematic depression of the curve for the width/length ratio with increasing distribution width, i.e., plumes are narrower and penetrate deeper for comparable Ω for wider distributions (Figure 4, right axis). This tendency for narrower plumes to form in wider distribution networks is preserved in the number of exiting fractures that carry flow (Figure 4, left axis) except near small Ω.

4. Conclusions

[9] The TBM augmented with dynamic overloading yields results that are similar to those obtained previously by I. In contrast, while the results of I were obtained by tuning the fraction of singly directed vs. splitting buckets, with dynamic overloading, divergent flow naturally occurs within the constrained ($\Phi = 1$) network. Additionally, inclusion of dynamic overloading captures temporal variation in pathway geometry, i.e., the formation of additional ephemeral pathways in time. Such transient behavior has been seen in the recent experiments of *Glass et al.* [2002] and *Wood et al.* [2004]. However, it is likely that yet-to-be-incorporated memory effects (e.g., pre-wetting) will be required to fully simulate flows in fracture networks. Such memory effects would include the possibility that an overloading event may change the original bias of the intersection; this is because capillary barriers are tipping points, and once they tip they may continue to split flow for a time, or flow entirely into the new branch. Finally, the formation of ephemeral transport pathways and other spatial temporal structure plays an important role in the reactive transport of contaminants in the subsurface.

[10] **Acknowledgments.** Supported by the INEEL Environmental Systems Research and Analysis Program and the Environmental Management Science Program, Office of Environmental Management, U.S. Dept. of Energy. The Idaho National Engineering & Environmental Laboratory is operated for the U.S. Dept. of Energy under DOE-ID Operations Office Contract DE-AC07-99ID13727. The Sandia National Laboratories are operated for the U.S. Dept. of Energy under DOE-AL Operations Office Contract DE-AC04-94AL85000.

References

Bonnet, E., O. Bour, N. E. Odling et al. (2001), Scaling of fracture systems in geological media, *Rev. Geophys.*, *39*, 347.

Coles, S. (2001), *An Introduction to Statistical Modeling of Extreme Values*, Springer-Verlag, New York.

Dhar, D., and R. Ramaswamy (1989), Exactly solved model of self-organized critical phenomena, *Phys. Rev. Lett.*, *63*, 1659.

Glass, R. J., and R. A. LaViolette (2004), Self organized spatio-temporal structure within the fractured Vadose Zone: Influence of fracture intersections, *Geophys. Res. Lett.*, *31*, L15501, doi:10.1029/2004GL019511.

Glass, R. J., M. J. Nicholl, S. E. Pringle, and T. R. Wood (2002), Unsaturated flow through a fracture-matrix-network: Dynamic preferential pathways in meso-scale laboratory experiments, *Water Resour. Res.*, *38*(12), 1281, doi:10.1029/2001WR001002.

Glass, R. J., M. J. Nicholl, H. Rajaram, and T. R. Wood (2003a), Unsaturated flow through fracture networks: Evolution of liquid phase structure, dynamics, and the critical importance of fracture intersections, *Water Resour. Res.*, *39*(12), 1352, doi:10.1029/2003WR002015.

Glass, R. J., H. Rajaram, and R. L. Detwiler (2003b), Immiscible displacements in rough-walled fractures: Competition between roughening by random aperture variations and smoothing by in-plane curvature, *Phys. Rev. E*, *68*, 061110.

Glass, R. J., M. J. Nicholl, H. Rajaram, and B. Andre (2004), Development of slender transport pathways in unsaturated fractured rock: Simulation with Modified Invasion Percolation, *Geophys. Res. Lett.*, *31*, L06502, doi:10.1029/2003GL019252.

LaViolette, R. A., R. J. Glass, T. R. Wood et al. (2003), Convergent flow observed in a laboratory-scale unsaturated fracture system, *Geophys. Res. Lett.*, *30*(2), 1083, doi:10.1029/2002GL015775.

Wood, T. R., M. J. Nicholl, and R. J. Glass (2002), Fracture intersections as integrators for unsaturated flow, *Geophys. Res. Lett.*, *29*(24), 2191, doi:10.1029/2002GL015551.

Wood, T. R., R. J. Glass, T. R. McJunkin et al. (2004), Unsaturated flow through a small fracture-matrix network: Part 1, Experimental observations, *Vadose Zone J.*, *3*, 90.

R. J. Glass, Sandia National Laboratories, Albuquerque, NM 87185-0735, USA.

R. A. LaViolette, Idaho National Engineering & Environmental Laboratory, Idaho Falls, ID 83415-2208, USA. (yaq@inel.gov)